PROCEEDINGS OF SCIENCE

New techniques for reconstructing and calibrating hadronic objects with ATLAS

Arnau Morancho Tardà [a,*] **, on behalf of the ATLAS Collaboration**

[a] *Niels Bohr Institue,*
University of Copenhagen, Denmark

E-mail: arnau.morancho.tarda@cern.ch

The precision and reach of physics analyses at the LHC are often tied to the performance of hadronic object reconstruction and calibration, with even small incremental gains in understanding and reduced uncertainties being impactful on ATLAS results. Recent refinements to the reconstruction and calibration procedures for jets and missing transverse momentum by the ATLAS collaboration have resulted in reduced uncertainties, improved pile-up stability, and overall performance gains. In this proceeding, we present highlights of these developments.

The European Physical Society Conference on High Energy Physics (EPS-HEP2025)
7-11 July 2025
Marseille, France

*Speaker

 ISSN 1824-8039 . Published by SISSA Medialab.

ATL-PHYS-PROC-2025-089
27/10/2025

PoS(EPS-HEP2025)242

1. Introduction

Hadronic objects play a central role in proton–proton collisions and are an essential component of nearly all experiments at the LHC [1]. Many measurements and searches rely directly on the performance of reconstructed jets and missing transverse momentum ($\mathbf{p}_{\mathrm{T}}^{\mathrm{miss}}$), while even those that do not depend on them explicitly must account for their impact on background modelling.

The reconstruction and calibration of jets are challenging due to their composite nature. Initiated by a single parton, they undergo parton showering, hadronisation, and decay before interacting with the detector. In this way, jets provide a global description of hadronic activity, while $p_{\mathrm{T}}^{\mathrm{miss}} = |\mathbf{p}_{\mathrm{T}}^{\mathrm{miss}}|$ quantifies the event's transverse momentum imbalance, often signalling the presence of non-interacting particles such as neutrinos or dark-matter candidates. Because $p_{\mathrm{T}}^{\mathrm{miss}}$ depends on all reconstructed objects, its accuracy is particularly sensitive to the calibration of hadronic activity.

Since Run 1, the calibration of jets and $p_{\mathrm{T}}^{\mathrm{miss}}$ in ATLAS [2] has undergone continuous refinement. The standard jet calibration chain is detailed in Refs. [3, 4], while new techniques continue to push performance and reduce uncertainties. Jets are reconstructed using the anti-k_t algorithm [5] with $R = 0.4$ (small-R) or $R = 1.0$ (large-R), and their energies and masses must be corrected for detector effects and contamination from additional interactions in the same bunch crossing. These multiple interactions, referred to as pile-up, remain a dominant challenge and are expected to intensify in the High-Luminosity LHC era. Limited calibration statistics and evolving running conditions further motivate the development of new strategies and techniques.

This note presents six novel approaches to improving the ATLAS jet and $p_{\mathrm{T}}^{\mathrm{miss}}$ calibration chain. These include a cell-time cut to suppress out-of-time pile-up [6], improved *in-situ* calibrations using single-particle E/p measurements [7] and pile-up–enriched dijet samples [8], machine-learning based calibrations for large-R [9] and b-jets [10], and new $p_{\mathrm{T}}^{\mathrm{miss}}$ working points optimised for pile-up conditions [11]. Together, these developments enhance the precision, stability, and robustness of jet and $p_{\mathrm{T}}^{\mathrm{miss}}$ reconstruction across the full Run 2 and beyond.

2. Reduced pile-up using calorimeter cell timing

Pile-up can occur in the same bunch crossing (in-time pile-up) or in neighbouring crossings (out-of-time pile-up), both affecting event reconstruction since bunches collide every 25 ns, shorter than the calorimeter's readout time.

Topo-clusters [12], built from calorimeter cells and later clustered into jets via the anti-k_t algorithm, currently use energy significance thresholds but no timing information. The study in Ref. [6] investigates the use of cell timing to suppress out-of-time pile-up already at the topo-clustering stage, reducing the impact of pile-up on jet reconstruction. The LAr and Tile calorimeter times are synchronised with the LHC clock to ensure a common time reference across all subdetectors. The cell time $|t_{\mathrm{cell}}|$ is computed if the cell energy exceeds the noise by $\sim 3\sigma$; otherwise it is set to zero.

Each calorimeter cell is assigned a signal significance $\zeta_{\mathrm{cell}}^{\mathrm{EM}} = E_{\mathrm{cell}}^{\mathrm{EM}}/\sigma_{\mathrm{noise,cell}}^{\mathrm{EM}}$, with clusters seeded by cells exceeding $\zeta_{\mathrm{cell}}^{\mathrm{EM}} > 4$, grown with neighbours above 2, and completed with neighbours above zero. Three timing-based variants were explored:

- Seed cut: cells with $\zeta_{\mathrm{cell}}^{\mathrm{EM}} > 4$ and $|t_{\mathrm{cell}}| < 12.5$ ns can seed.

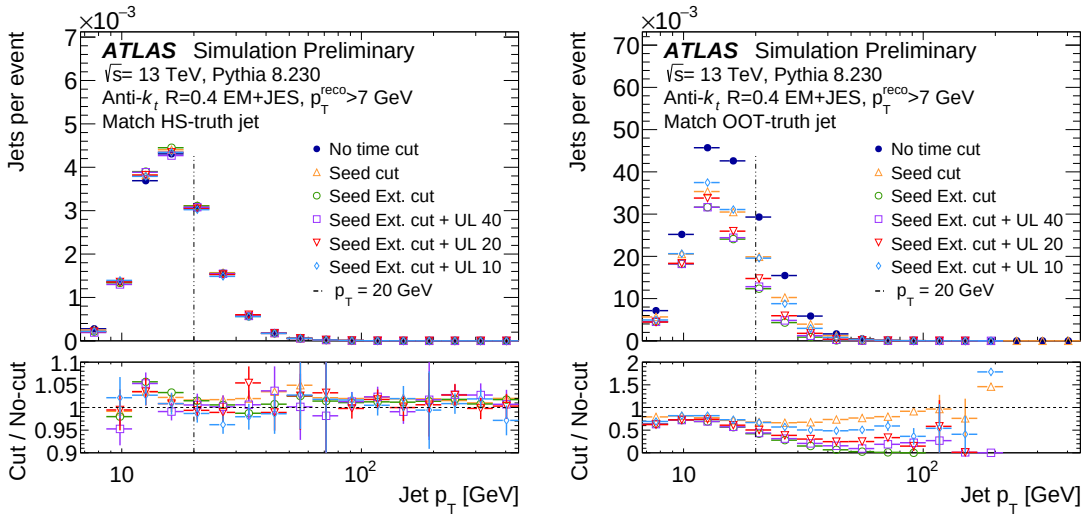

Figure 1: Number of selected jets per event matched to a truth jet as a function of p_{T}, for different calorimeter cell timing cuts applied in the topo-clustering algorithm. Left: hard-scatter truth jets. Right: out-of-time pile-up truth jets. The lower panels show the ratios with respect to the no-cut case. Plots from Ref. [6].

- Seed Extended: cells failing the time cut are excluded entirely from clustering.
- Seed Extended UpperLimit: cells failing the cut can still seed if $\zeta_{\mathrm{cell}}^{\mathrm{EM}}$ exceeds a threshold $X_{UL} = (10, 20, 40)$, ensuring possible long-lived particle signals are retained.

Simulation studies in Run 2 (Figure. 1) show that stricter cuts substantially reduce out-of-time pile-up jets while preserving hard-scatter jets. The Seed Extended cut outperforms the Seed cut, offering more effective pile-up suppression, whereas the UpperLimit with $X_{UL} = 10$ is too loose. The *Seed Extended UpperLimit* with $X_{UL} = 20$ achieves the best balance, reducing out-of-time pile-up jets by ∼50% for $p_{\mathrm{T}} \sim 20$ GeV and ∼80% for $p_{\mathrm{T}} \geq 50$ GeV. Potential long-lived particle signatures can be addressed later with dedicated selections. This configuration is now the ATLAS Run 3 Topo-cluster default, also reducing disk usage by 6% in data and 7% in simulation.

3. Improvements to jet calibration using alternative event samples

Jets require a precise calibration of their energy response for accurate physics analyses. Two complementary, data-driven approaches have been developed to improve the accuracy of jet energy calibration: one based on the calorimeter response to isolated single particles, and another exploiting pile-up events as a source of low-energy hadronic jets. Together, they enhance the precision of both the jet energy scale (JES) and the jet energy resolution (JER) across a wide p_{T} range of small-R jets.

The single-particle method [13, 14] measures the ratio between the energy deposited in the calorimeter (E) and the momentum (p) measured by the inner detector, known as the E/p ratio. Since jets are superpositions of many particle deposits, a deconvolution method is used to propagate the single-particle response to jets. After correcting and smearing the calorimeter energy deposits, data-to-MC correction factors are extracted. This provides a direct measurement of the calorimeter

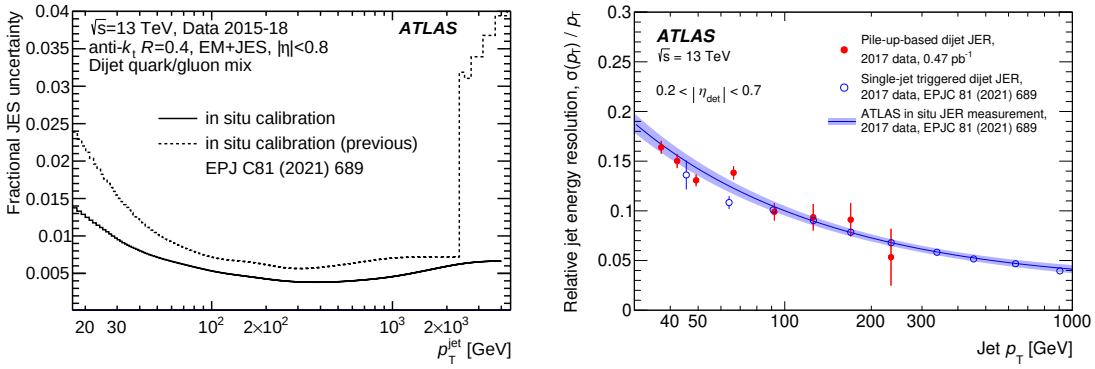

Figure 2: Left: Jet energy scale (JES) uncertainty obtained with the E/p single-particle method (solid line) compared to previous results (dashed line); from Ref. [7]. Right: Jet energy resolution (JER) as a function of p_{T} using the dijet balance method for single-jet triggered (open blue dots) and with the pile-up dataset (filled red dots) for 2017 data; from Ref. [8].

response to charged hadrons and therefore a means to constrain the JES uncertainty. In Run 1, the method relied on low pile-up minimum-bias data with single-particle momenta below 10 GeV [14]. The resulting JES was consistent with the p_{T}-balance technique but had larger uncertainties, limiting its applicability.

In Run 2, the approach was significantly extended using isolated pions from hadronic τ decays in W boson events, covering a broad p_{T} range of 10–300 GeV [15]. Building on this, the study in Ref. [7] derives the JES and its uncertainty using the E/p method and compares the results with other established techniques. The JES obtained with this approach is in good agreement with the p_{T}-balance method, and being uncorrelated, their combination reduces the total JES uncertainty. In particular, for EMTopo small-R jets in Run 2 (left panel of Figure 2), the uncertainty reaches 0.3% at $p_{\mathrm{T}} = 300$ GeV and 0.4% at 4 TeV, compared to 4.0% in earlier studies. The same technique is also applied to other jet definitions, such as particle-flow jets, different radius parameters, or quark- and gluon-initiated jets.

While the E/p method improves the calibration of high-precision JES measurements, a complementary strategy targets the low-p_{T} regime of the JER. The JER describes the spread of the reconstructed jet p_{T} with respect to its true value and can be parameterised as $\sigma(p_{\mathrm{T}})/p_{\mathrm{T}} = N/p_{\mathrm{T}} + S/\sqrt{p_{\mathrm{T}}} + C$, where N, S, and C represent the noise, stochastic, and constant terms, respectively. Traditionally, it is determined using transverse momentum balance in dijet events, but at low p_{T} such events are strongly limited by prescaled triggers. The random-cone method [3] is used to partially constrain the noise term.

To improve statistical limitations of dijet events, the study in Ref. [8] explores pile-up events as a trigger-unbiased source of dijets. Events selected with a single-lepton trigger allow for an easier removal of the hard-scatter interaction, leaving clean dijet topologies originating from pile-up vertices. Although the efficiency of selecting at least one good pile-up vertex that satisfies all criteria is only about 2%, the high rate compensates for the low selection efficiency. The dijet balance method is then applied to the pile-up sample, combined with the standard dijet dataset. As shown in the right panel of Figure 2, the inclusion of pile-up dijets provides additional low-p_{T} bins

with reduced statistical uncertainty, improving the precision of the JER measurement. In particular, for $p_{\mathrm{T}}^{\mathrm{lead}} < 60$ GeV, the uncertainty on the noise term N decreases by about 40%, and on the stochastic term S by about 20%.

4. Machine learning approaches to jet calibration

Machine learning techniques enable multidimensional jet calibration by learning correlations between observables and exploiting low-level detector information. Recent developments include deep neural networks (DNNs) for the simultaneous energy–mass calibration of Large-R jets [9] and transformer networks for constituent-based b-jet calibration [10].

Large-R jets ($R = 1.0$) are used to reconstruct boosted objects, where the decay products are collimated and can be clustered within a single jet. For these jets, it is important to measure both the jet energy and jet mass accurately, since the reconstructed mass should be close to that of the original object.

In the study detailed in Ref. [9], a DNN is trained to derive both the jet energy and mass scales (JES and JMS) while improving the corresponding resolutions (JER and JMR). The model uses the *unified flow object* (UFO) jet collection [16] and includes some specific architectural features: a mixture-density-network loss to better regress Gaussian-like response distributions, an η-annotation step to capture η-dependent variations, and a residual connection in the mass branch to stabilise convergence. Trained on simulated QCD dijets and validated on W/Z, Higgs, and top-quark samples, the DNN achieves a more stable jet energy response while improving the jet energy resolution by about 30% for $p_{\mathrm{T}} > 500$ GeV (left panel of Figure 3), with similar gains for the jet mass. It also shows reduced pile-up sensitivity, improved flavour robustness, and smaller non-closure across different MC generators.

Transformer-based networks detailed in Ref. [10] extend this concept to constituent-level calibration of b-jets, where displaced vertices, semileptonic decays, and missing neutrinos affect the reconstructed response. Such effects have traditionally been mitigated using dedicated correction tools: the *muon-in-jet* correction, which adds the muon momentum to that of the jet, and the *PtReco* correction, which applies a p_{T}-dependent adjustment for residual response differences [17]. While effective, these approaches handle only specific effects, whereas machine learning offers a unified, data-driven solution. Separate transformer models are trained for small-R and large-R jets, using constituent, track, and (for small-R jets) soft-lepton features. The architectures are inspired by transformer networks developed for jet tagging [18, 19], but instead of classification, they perform regression of the jet energy and, for Large-R jets, also the jet mass response. After processing the inputs through transformer encoder layers and attention pooling, the network predicts the calibrated jet response using a mean absolute error loss.

For small-R b-jets, the transformer calibration yields a more stable response around unity and improves the energy resolution by 18–31%, translating into an approximate 22% improvement in the reconstructed Higgs and Z boson mass resolution. For large-R b-jets, both energy and mass responses are more linear and stable, with resolution gains of 25–35% in energy and 26–33% in mass. This leads to improved reconstructed mass peaks by 10–15% for Z and top quarks, and about 10% for Higgs bosons, as shown on the right panel of Figure 3. Overall, the transformer-based

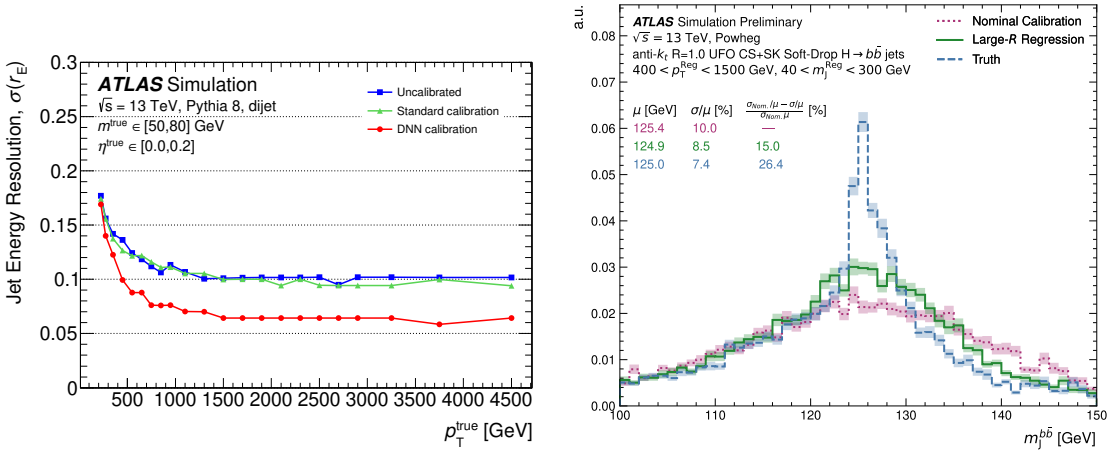

Figure 3: Left: Jet energy resolution as a function of p_T for Large-R jets on Run2 simulation data using the DNN calibration (red) compared to the standard sequential correction method (green); from Ref. [9]. Right: Reconstructed Higgs boson mass distribution as a function of p_T for Large-R b-jets on Run2 simulation data: truth (blue dashed), nominal calibration (pink dotted), and the transformer regression model (solid green); from Ref. [10].

calibration provides a unified approach that simultaneously corrects multiple correlated effects, outperforming traditional sequential corrections.

5. Performance of missing transverse momentum reconstruction

The reconstruction of p_T^{miss} in ATLAS relies on all calibrated physics objects in the event, complemented by a *soft term* built from tracks not associated with them. It is defined as the negative vector sum of all visible transverse momenta, reflecting overall momentum conservation. True p_T^{miss} originates from undetected particles such as neutrinos or hypothetical dark-matter candidates, whereas detector inefficiencies and energy mismeasurements produce fake p_T^{miss}. As jets dominate the uncertainties in p_T^{miss}, accurate jet calibration is essential.

The latest ATLAS results in Ref. [11] use the full Run 2 dataset to improve the performance of these objects. The soft term is computed with a track-based approach, improving pile-up robustness; four working points (Loose, Tight, Tighter, and Tenacious) are defined with increasingly stringent jet p_T and Jet Vertex Tagger (JVT) requirements [20]. The recommended Tight WP applies JVT > 0.5 for jets with $p_T < 60$ GeV and $|\eta| < 2.4$, and p_T thresholds of 20 GeV (central) and 35 GeV (forward). With this configuration, scale and resolution uncertainties are reduced by up to 76% and 51% relative to 2015 results [21]. Maintaining multiple working points allows analyses to balance efficiency and pile-up resilience as needed.

The p_T^{miss} reconstruction is commonly evaluated using $Z \to \mu\mu$ events, where true p_T^{miss} is minimal and reconstructed imbalance reflects detector effects or background processes with neutrinos. Figure 4 shows good agreement between data and simulation: the $Z \to \mu\mu$ sample (pink) peaks at low p_T^{miss}, while processes such as diboson events (light blue) for example populate higher values. An additional improvement is the introduction of an object-based significance, which uses the covariance of reconstructed objects to enhance discrimination against fake p_T^{miss}.

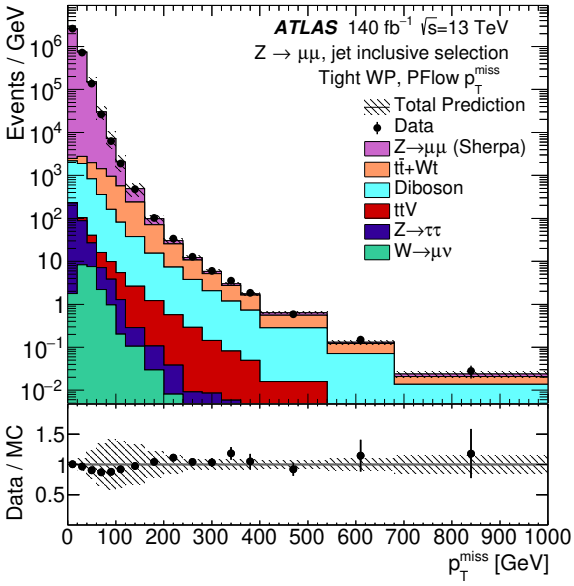

Figure 4: Distribution of $p_{\mathrm{T}}^{\mathrm{miss}}$ for a $Z \to \mu\mu$ selection, comparing data and simulation in Run 2 for the Tight WP. Plot from Ref. [11].

6. Conclusions

At the LHC, and in particular within the ATLAS experiment, hadronic objects play a crucial role in many physics analyses, and a precise reconstruction of the missing transverse momentum is essential for searches for Beyond Standard Model physics.

In this proceeding, a summary of six notes [6–11] describing new methods to improve the reconstruction and calibration of hadronic objects has been presented. Each method targets different parts of the calibration chain for jets and missing transverse momentum, proposing specific solutions to enhance their performance.

A cell-timing cut has been implemented in Run 3 to reduce out-of-time pile-up at early stages of the reconstruction, consequently lowering the required disk space. In addition, new samples have been explored, such as isolated pion measurements to reduce the JES systematics, and pile-up dijet events to increase the statistical power of the dijet method for low-p_{T}. The use of machine learning techniques improves the Monte Carlo calibration of large-R jets by approximately 30% in both energy and mass resolution, while a dedicated ML-based calibration for b-jets enhances the mass resolution of heavy bosons, such as H or Z, by about 22% (10–15%) for small-R (large-R) jets. Finally, new working points for missing transverse momentum, optimised for different pile-up conditions and jet kinematics, have been explored to improve its performance across various scenarios.

Continuous developments in reconstruction and calibration techniques are being pursued to further enhance the performance of hadronic objects at ATLAS, ensuring robust and precise measurements for current and future physics analyses.

References

[1] L. Evans and P. Bryant, eds., *LHC Machine*, *JINST* **3** (2008) S08001.

[2] ATLAS Collaboration, *The ATLAS Experiment at the CERN Large Hadron Collider*, *JINST* **3** (2008) S08003.

[3] ATLAS Collaboration, *Jet energy scale and resolution measured in proton–proton collisions at* $\sqrt{s}$ = 13 *TeV with the ATLAS detector*, *The European Physical Journal C* **81** (2021) .

[4] ATLAS Collaboration, *In situ calibration of large-radius jet energy and mass in 13 TeV proton–proton collisions with the ATLAS detector*, *The European Physical Journal C* **79** (2019) .

[5] M. Cacciari, G.P. Salam and G. Soyez, *The anti-*k_t *jet clustering algorithm*, *JHEP* **04** (2008) 063 [0802.1189].

[6] ATLAS Collaboration, *Improving topological cluster reconstruction using calorimeter cell timing in ATLAS*, *The European Physical Journal C* **84** (2024) .

[7] ATLAS Collaboration, *A precise measurement of the jet energy scale derived from single-particle measurements and in situ techniques in proton–proton collisions at* $\sqrt{s}$ = *13 TeV with the ATLAS detector*, *The European Physical Journal C* **85** (2025) .

[8] ATLAS Collaboration, *Using pile-up collisions as an abundant source of low-energy hadronic physics processes in ATLAS and an extraction of the jet energy resolution*, *Journal of High Energy Physics* **2024** (2024) .

[9] ATLAS Collaboration, *Simultaneous energy and mass calibration of large-radius jets with the ATLAS detector using a deep neural network*, *Machine Learning: Science and Technology* **5** (2024) 035051.

[10] ATLAS Collaboration, *Transformer networks for constituent-based b-jet calibration with the ATLAS detector*, Tech. Rep. CERN, Geneva (2024).

[11] ATLAS Collaboration, *The performance of missing transverse momentum reconstruction and its significance with the ATLAS detector using 140* fb^{-1} *of* $\sqrt{s}$ = 13 *TeV pp collisions*, *The European Physical Journal C* **85** (2025) .

[12] ATLAS Collaboration, *Topological cell clustering in the ATLAS calorimeters and its performance in LHC Run 1*, *The European Physical Journal C* **77** (2017) .

[13] ATLAS Collaboration, *Single hadron response measurement and calorimeter jet energy scale uncertainty with the ATLAS detector at the LHC*, *The European Physical Journal C* **73** (2013) .

[14] ATLAS Collaboration, *A measurement of the calorimeter response to single hadrons and determination of the jet energy scale uncertainty using LHC Run 1 pp-collision data with the ATLAS detector*, *The European Physical Journal C* **77** (2017) .

[15] ATLAS Collaboration, *Measurement of the energy response of the ATLAS to charged pions from $W^{\pm} \to \tau^{\pm}(\to \pi^{\pm}\nu_{\tau})\nu_{\tau}$ events in Run 2 data*, The European Physical Journal C **82** (2022) .

[16] ATLAS Collaboration, *Optimisation of large-radius jet reconstruction for the ATLAS detector in TeV proton–proton collisions*, The European Physical Journal C **81** (2021) .

[17] ATLAS Collaboration, *Evidence for the $H \to b\bar{b}$ decay with the ATLAS detector*, Journal of High Energy Physics **2017** (2017) .

[18] ATLAS Collaboration, *Graph Neural Network Jet Flavour Tagging with the ATLAS Detector*, Tech. Rep. , CERN, Geneva (2022).

[19] ATLAS Collaboration, *Transformer Neural Networks for Identifying Boosted Higgs Bosons decaying into $b\bar{b}$ and $c\bar{c}$ in ATLAS*, Tech. Rep. , CERN, Geneva (2023).

[20] ATLAS Collaboration, *Performance of pile-up mitigation techniques for jets in pp collisions at $\sqrt{s} = 8$ Tev using the atlas detector*, The European Physical Journal C **76** (2016) .

[21] ATLAS Collaboration, *Performance of missing transverse momentum reconstruction with the ATLAS detector using proton–proton collisions at $\sqrt{s} = 13$ TeV*, The European Physical Journal C **78** (2018) .